

Mononuclear chromium(III), manganese(II) and iron(III) complexes of the pentadentate ligand 1,4-bis(2-pyridylmethyl)-1,4,7-triazacyclononane †

Gary D. Fallon, Grant A. McLachlan, Boujemaa Moubaraki, Keith S. Murray, Lynda O'Brien and Leone Spiccia *

Department of Chemistry, Monash University, Clayton, Victoria 3168, Australia

Chromium(III), manganese(II) and iron(III) complexes of dmptacn [1,4-bis(2-pyridylmethyl)-1,4,7-triazacyclononane] with general formula $[M(dmptacn)Cl]^{n+}$ have been prepared by reaction of the macrocycle with the corresponding metal chloride salts and their physicochemical properties examined. Magnetic susceptibility, Mössbauer and ESR measurements have shown that the iron(III) complex $[Fe(dmptacn)Cl][PF_6]_2 \cdot MeOH$ exhibits spin-crossover behaviour, existing in the low-spin form below 50 K and as a mixture of low- and high-spin forms at 298 K. The structure of $[Cr(dmptacn)Cl][ClO_4]_2$ confirmed that the isomer formed has the secondary nitrogen adjacent to the chloro ligand and that there is significant distortion from octahedral geometry in the complex, both common features of complexes of dmptacn. Two enantiomeric forms of the complex are found in the unit cell, *vis-à-vis* in one enantiomer the $\delta\delta\delta$ conformation of the tacn ring is coupled with a $\lambda\lambda$ conformation of the pyridyl arms while the opposite conformations are observed in the other.

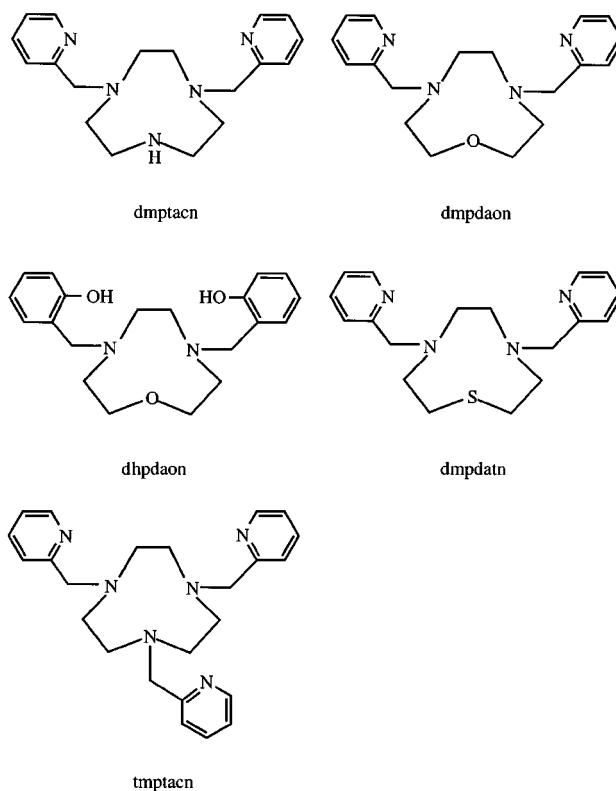
The co-ordination chemistry of 1,4,7-triazacyclononane (tacn) and N-functionalised derivatives of tacn has been examined in considerable detail over the last two decades and their application in many diverse aspects of modern co-ordination chemistry reported.¹ A number of pentadentate ligands, with pendant arms attached to two nitrogens on tacn, have been studied but these remain relatively rare compared with hexadentate ligands, with arms attached to all three nitrogens.¹ The complexation of pentadentate derivatives of tacn and the related macrocycles 1-thia-4,7-diazacyclononane (datn) and 1-oxa-4,7-diazacyclononane (daon) has been dominated by the complexes of copper(II), nickel(II) and cobalt(III) with less emphasis on chromium, manganese and iron. Nevertheless, two pentadentate derivatives of daon have been used to prepare iron complexes. The dhpdaon ligand of Flassbeck and Wiegardt² forms high-spin, octahedral iron(III) complexes, $[FeL(X)]^{2+}$ ($X = Cl^-$, N_3^- , NCS^- or MeO^-). Szulbinski *et al.*³ report the preparation of the low-spin, octahedral iron(II) complex $[Fe(dmtpdaon)Cl]PF_6$, where dmtpdaon is 4,7-bis(2-pyridylmethyl)-1-oxa-4,7-diazacyclononane. These workers⁴ also used the complex to gain an insight into the disproportionation of the biologically harmful superoxide ion. Reactivity studies have shown that this iron(II) complex does not react with dioxygen but it does react with superoxide to give an adduct best formulated as an iron(III) peroxide, rather than an iron(II) superoxide species.

As part of ongoing investigations of pentadentate ligands, we have been examining the co-ordination chemistry of 1,4-bis(2-pyridylmethyl)-1,4,7-triazacyclononane (dmptacn)⁵⁻⁷ and related bis(pentadentate) binucleating ligands.⁸ Reported here are the syntheses and physicochemical properties of chromium(III), manganese(II) and iron(III) complexes of this ligand. Of particular interest has been the spin-crossover behaviour of $[Fe(dmptacn)Cl][PF_6]_2 \cdot MeOH$ since iron(III) spin-crossover compounds⁹ are less common than those of iron(II).¹⁰

Experimental

Reagents and materials

Reagent-grade materials or better were used throughout this



work. The compound dmptacn was prepared by a published method.⁵

CAUTION: although no problems were encountered in this work, transition-metal perchlorates are potentially explosive and should be prepared in small quantities.

Physical measurements

Infrared spectra were recorded on a Perkin-Elmer 1600 FT-IR spectrometer as KBr pellets and electronic spectra on either a Hitachi 150-20 or a Cary 3 spectrophotometer. The instrumentation for electron microprobe analyses and details of sample preparation have been described previously.⁶ Microanalyses were performed by Chemical and Micro-Analytical Services

† Non-SI unit employed: $\mu_B \approx 9.27 \times 10^{-24} \text{ JT}^{-1}$

(CMAS) of Melbourne, Australia. Room-temperature magnetic moments were determined by the Faraday method and diamagnetic corrections made using Pascal's constants. Variable-temperature (4.2–300 K) magnetic susceptibility measurements were carried out on a Quantum Design MPMS SQUID magnetometer as described elsewhere.⁵ Cyclic voltammograms were measured in dry, deoxygenated acetonitrile (*ca.* 10^{-3} mol dm⁻³ with 0.1 mol dm⁻³ NBu₄ClO₄ as supporting electrolyte) using a BAS-100 instrument connected to a three-electrode cell consisting of a glassy carbon working electrode, a platinum-wire auxiliary electrode and a Ag–AgCl reference electrode. Electron spin resonance spectra in frozen dimethylformamide (dmf)–MeOH solution (77 K) were recorded in iron-free quartz tubes using a Varian E12 spectrometer operating at X-band frequency (9.11 GHz). Mössbauer spectra were obtained in the transmission mode using a ⁵⁷Co in rhodium source and were recorded in the absence of an applied magnetic field. The data were fitted by Lorentzian line shapes using a least-squares procedure.

Syntheses

[Cr(dmptacn)Cl][ClO₄]₂. Chromium(III) chloride (0.30 g, 2.4 mmol) was added to a solution of dmptacn (0.76 g, 2.4 mmol) in methanol (150 cm³) under nitrogen and the solution stirred for 15 min. After the nitrogen flow was stopped, the solution was diluted to 1.4 dm³ with water and adsorbed onto a Bio-Rad AG 50W-X2 cation-exchange column and the column washed thoroughly with water. Elution with 1.5 mol dm⁻³ HCl removed a single red band which was concentrated and NaClO₄ (1.6 g) added. The red precipitate that formed on standing was filtered off and washed with ethanol. Yield 1.14 g, 79%. Slow evaporation of the filtrate gave crystals suitable for crystallography (Found: C, 36.1; H, 4.2; N, 11.4. Calc. for C₁₈H₂₅Cl₃CrN₅O₈: C, 36.2; H, 4.2; N, 11.7%). Microprobe analysis: Cr:Cl ratio 1:3. IR (cm⁻¹): 3243m (NH), 1610s, 1468m, 1444m (pyridine ring), 1091vs, 625m (ClO₄⁻).

[Mn(dmptacn)(H₂O)][ClO₄]₂. The compound MnCl₂·4H₂O (0.48 g, 2.4 mmol) was added to a solution of dmptacn (0.76 g, 2.4 mmol) in methanol (125 cm³) and stirred for 15 min before adding NaClO₄ (1.0 g). Storage of the solution at 4 °C overnight gave a pale yellow precipitate which was filtered off and washed with ethanol. Yield 1.03 g, 73% (Found: C, 36.0; H, 4.6; N, 11.8. Calc. for C₁₈H₂₇Cl₂N₅O₉: C, 36.0; H, 4.8; N, 11.7%). Microprobe analysis: Mn:Cl ratio 1:2. IR (cm⁻¹): 3422m (OH), 3326m (NH), 1607s, 1484m, 1441s (pyridine ring), 1088vs, 626m (ClO₄⁻).

[Fe(dmptacn)Cl][PF₆]₂·MeOH. The compound FeCl₃·6H₂O (0.66 g, 2.4 mmol) was added to a solution of dmptacn (0.76 g, 2.4 mmol) in methanol (60 cm³). The solution was refluxed for 3 h, after which a solution of NH₄PF₆ (0.80 g, 5 mmol) in methanol (*ca.* 20 cm³) was added. A brown precipitate formed on storage of the solution at 4 °C overnight. It was filtered off and washed with ethanol. Yield 1.21 g, 69% (Found: C, 32.0; H, 4.0; N, 9.7. Calc. for C₁₈H₂₅ClF₁₂N₅P₂·CH₃OH: C, 31.5; H, 4.0; N, 9.7%). Microprobe analysis: Fe:Cl:P ratio 1:1:2. IR (cm⁻¹): 3440m (OH), 3222m (NH), 1613s, 1474m, 1448m (pyridine ring), 837vs (PF₆⁻).

Crystallography

A representative crystal of approximate dimensions (0.35 × 0.16 × 0.31 mm) was used for data collection. Intensity measurements were made on a Phillips PW1100 diffractometer using graphite-monochromated Mo-K α radiation with $6 < 2\theta < 60^\circ$, operating in a ω -scan mode with a scan range of $\pm(0.75 + 0.15 \tan \theta)^\circ$, at a scan rate of $0.04^\circ \text{ s}^{-1}$. Three standard reflections monitored every 4 h showed no significant variation in intensity over the data collection period. Intensity data were

processed as described previously¹¹ and a face-indexed numerical absorption correction applied.¹² The atomic scattering factors for neutral atoms were taken from ref. 13 and corrected for anomalous dispersion by using values from ref. 13. The SHELX 76 program was used for least-squares refinement. The structure was solved by direct methods. Refinement (based on *F*) was by full-matrix least squares employing anisotropic thermal parameters for Cr, Cl and O, and isotropic thermal parameters for all other atoms (single isotropic thermal parameter for hydrogen which refined to 0.059 \AA^2 ; positioned in geometrically idealised positions C–H 0.97 Å).

Crystallographic data, selected bond distances and angles are given in Tables 1 and 2, Fig. 1 shows the structure of the cation and atomic labelling scheme.

Atomic coordinates, thermal parameters, and bond lengths and angles have been deposited at the Cambridge Crystallographic Data Centre (CCDC). See Instructions for Authors, *J. Chem. Soc., Dalton Trans.*, 1997, Issue 1. Any request to the CCDC for this material should quote the full literature citation and the reference number 186/573.

Results and Discussion

Synthesis of complexes

The synthesis of [Mn(dmptacn)(H₂O)][ClO₄]₂ and [Fe(dmptacn)Cl][PF₆]₂·MeOH involved direct reaction of the ligand with hydrated metal chlorides in methanol followed by addition of NaClO₄ or NH₄PF₆, respectively. The chromium(III) complex [Cr(dmptacn)Cl][ClO₄]₂ was prepared by treating equimolar amounts of dmptacn and CrCl₃ in water under nitrogen to give a chromium(III) complex which is rapidly oxidised on exposure to atmospheric oxygen. Cation-exchange chromatography gave a single red band from which the product could be precipitated following concentration and addition of NaClO₄. The IR spectrum of these products exhibited a single NH stretching band in the 3220–3250 cm⁻¹ region and bands due to the ring stretching vibrations of the pyridyl groups at *ca.* 1610, 1470 and 1440 cm⁻¹, indicating incorporation of dmptacn into the complexes.

Crystal structure of [Cr(dmptacn)Cl][ClO₄]₂

The molecular structure of the [Cr(dmptacn)Cl]²⁺ cation, Fig. 1, shows that the geometry about the Cr^{III} is pseudo-octahedral, with five sites occupied by the nitrogen donors of dmptacn and a chloride ion completing the co-ordination sphere. Strong facial co-ordination of the tacn moiety results in similar bond angles and distances, within this portion of the ligand, to those found in other chromium(III) complexes of tacn derivatives with different pendant arms. Thus, the Cr–N (tacn) distances, 2.047(6), 2.058(5) and 2.073(5) Å, and N–Cr–N bite angles to the tacn nitrogens match those in (1,4,7-triazacyclononane-1,4,7-triacetato)chromium(III).¹⁴ The Cr–N (pyridine) bond distances [Cr–N(4) 2.062(5) and Cr–N(5) 2.065(5) Å] are shorter than normal [average 2.146(8) Å].¹⁵ The Cr^{III}–Cl distances [2.295(2) Å] are typical [average 2.309(7) Å].¹⁵ The distortion from the regular octahedral geometry, due to the fact that the tacn ring is not quite large enough to occupy three corners in a regular octahedron, is larger than that in [Co(dmptacn)(H₂O)][ClO₄]₃.⁷ In the latter the smaller cobalt(III) ion allows the ligand to approach a more regular octahedral geometry. In keeping with this, the angles subtended by the chelate rings formed by the tertiary amines and the pyridyl nitrogens in [Cr(dmptacn)Cl][ClO₄]₂ (average 80.6°) are more acute than the corresponding angles in [Co(dmptacn)(H₂O)][ClO₄]₃ (average 85.2°).

Although the [Cr(dmptacn)Cl]²⁺ complex can form in either of two geometric isomers (A and B in Fig. 2), the isomer observed has the chloride *cis* to the secondary amine, *i.e.* A. The five-membered chelate rings of the tacn backbone can adopt either the $\lambda\lambda\lambda$ or $\delta\delta\delta$ conformation. The five-membered chelate

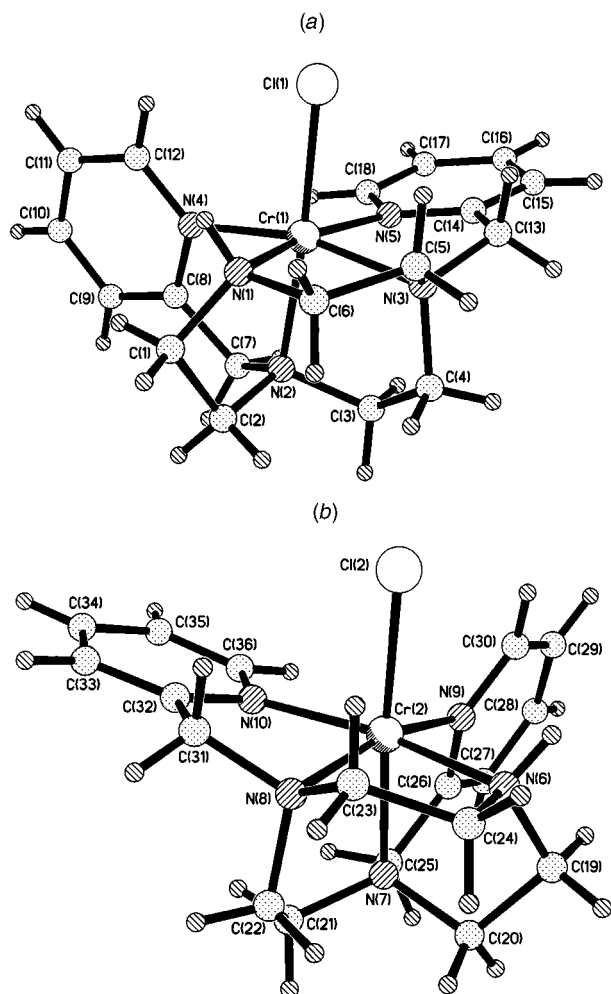


Fig. 1 Molecular structure and labelling scheme for the two cations in $[\text{Cr}(\text{dmptacn})\text{Cl}][\text{ClO}_4]_2$

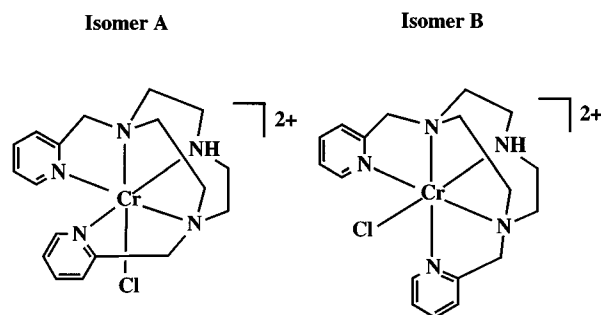


Fig. 2 Geometric isomers of $[\text{Cr}(\text{dmptacn})\text{Cl}]^{2+}$

rings formed by co-ordination of the two pyridyl arms to Cr^{III} can also have δ and λ conformations. If the tacn conformation is $\delta\delta\delta$, these rings adopt the λ conformation. Since the complex crystallises in a centrosymmetric space group, the two enantiomers are present in the unit cell and thus crystals of $[\text{Cr}(\text{dmptacn})\text{Cl}][\text{ClO}_4]_2$ are racemic. The second enantiomer has the tacn moiety in the $\lambda\lambda\lambda$ conformation with the pyridyl pendant arms in the δ conformation.

Considerable trigonal twisting of the pyridine nitrogens relative to the tacn nitrogens is found in the complex indicating significant distortion from octahedral geometry. The pyridines are rotated by 15° from the expected 60° ($\theta = 45^\circ$). The chloride ligand, however, is located at the expected position for ideal octahedral geometry. The θ angles in $[\text{Cr}(\text{dmptacn})\text{Cl}]^{2+}$ are smaller than in $[\text{Co}(\text{dmptacn})(\text{H}_2\text{O})]^{3+}$,⁷ indicating greater distortion from octahedral geometry in the former. This observation is in agreement with data for a series of tmptacn complexes where it was found that distortion towards trigonal-

Table 1 Crystallographic data for $[\text{Cr}(\text{dmptacn})\text{Cl}][\text{ClO}_4]_2$

Chemical formula	$\text{C}_{18}\text{H}_{25}\text{CrCl}_3\text{N}_5\text{O}_8$
<i>M</i>	597.8
Crystal system	Triclinic
Space group	$\bar{P}1$ (no. 2)
<i>a</i> /Å	23.053(7)
<i>b</i> /Å	11.318(2)
<i>c</i> /Å	9.477(3)
α /°	98.75(2)
β /°	102.00(1)
γ /°	90.33(1)
<i>V</i> /Å ³	2389(1)
<i>Z</i>	4
<i>T</i> /K	293(1)
λ /Å	0.710 69 (Mo-K α)
<i>D_c</i> , <i>D_m</i> /g cm ⁻³	1.66, 1.68(1)
<i>F</i> (000)	1228
μ (Mo-K α)/cm ⁻¹	8.6
Transmission factor range	0.747–0.864
$2\theta_{\text{max}}$ /°; <i>hkl</i> data collected	60; $\pm h, \pm k, \pm l$
No. data measured	14 652
No. unique data	13 887
No. observed data [$I \geq 3\sigma(I)$]	6289
No. parameters refined	402
<i>R</i> ^a	0.069
<i>R</i> ' ^b	0.068
Goodness of fit ^c	2.18
Maximum Δ/σ	0.079
Maximum $\Delta\rho/e \text{ \AA}^{-3}$	0.87

^a $R(F) = \sum(|F_o| - |F_c|)/\sum|F_o|$. ^b $R' = [\sum w(|F_o| - |F_c|)^2]^{1/2}$, $w = [\sigma^2(F_o)]^{-1}$.
^c $[\sum w(|F_o| - |F_c|)^2 / (N_{\text{observed}} - N_{\text{parameter}})]^{1/2}$.

prismatic geometry becomes more pronounced as the radius of the metal ion increases.^{16,17}

Physicochemical properties

Physicochemical data for complexes of dmptacn and related ligands are listed in Table 3. The electronic spectrum of $[\text{Cr}(\text{dmptacn})\text{Cl}][\text{ClO}_4]_2$ in acetonitrile is typical of a $\text{Cr}^{\text{III}}\text{N}_5\text{Cl}$ chromophore. Bands at 506 and 381 nm correspond to transitions from the ${}^4\text{A}_{2g}(\text{O}_h)$ ground state to ${}^4\text{T}_{2g}(\text{v}_1)$ and ${}^4\text{T}_{1g}(\text{F})$ states (v_2), respectively. The ligand-field parameter $10Dq = 19\,800 \text{ cm}^{-1}$ and Racah parameter $B = 615 \text{ cm}^{-1}$ were calculated from the spectrum. The 33% reduction in *B* from the free-ion value is typical for chromium(III) amine complexes.¹⁸ The value of $10Dq$ indicates that the N_5Cl chromophore exerts a weaker ligand field than the N_6 chromophore in $[\text{Cr}(\text{tmptacn})]^{3+}$ ($10Dq = 21\,100 \text{ cm}^{-1}$),¹⁷ $[\text{Cr}(\text{tacn})_2]^{3+}$ ($10Dq = 22\,800 \text{ cm}^{-1}$)¹⁹ and $[\text{Cr}(\text{dtne})_2]^{3+}$ [$10Dq = 20\,800 \text{ cm}^{-1}$, dtne = 1,2-bis(1,4,7-triazacyclonon-1-yl)ethane].²⁰ The electronic spectrum of $[\text{Fe}(\text{dmptacn})\text{Cl}]^{2+}$ in acetonitrile is different to that of the related low-spin complex $[\text{Fe}(\text{tmptacn})]^{3+}$ (Table 3). Apart from the expected $\pi \rightarrow \pi^*$ transition within the pyridyl rings, the spectrum of $[\text{Fe}(\text{dmptacn})\text{Cl}]^{2+}$ is dominated by a quite intense charge-transfer band at 430 nm attributable to either a Fe^{III} (low spin) \rightarrow pyridyl or a $\text{Cl}^- \rightarrow \text{Fe}^{\text{III}}$ (high spin) transition.

The room-temperature magnetic moments, μ_{eff} , of the complexes of Cr^{III} and Mn^{II} are normal for Cr^{III} and high-spin Mn^{II} . The moment for $[\text{Fe}(\text{dmptacn})\text{Cl}][\text{PF}_6]_2 \cdot \text{MeOH}$ of $3.58 \mu_{\text{B}}$ is intermediate between that for high- ($\mu_{\text{SO}} = 5.92 \mu_{\text{B}}$) and low-spin ($\mu_{\text{SO}} = 1.73 \mu_{\text{B}}$) electronic configurations. Thus this complex could be an intermediate-spin ($S = \frac{3}{2}$) complex or one exhibiting spin-crossover behaviour observed when $10Dq$ is approximately equal to the pairing energy. The latter situation was confirmed by variable-temperature susceptibility measurements which showed a dramatic drop in μ_{eff} between 300 and 180 K to a plateau value of *ca.* $2.1 \mu_{\text{B}}$ (Fig. 3), a value typical of low-spin Fe^{III} .^{17,19,20} Thus, the complex is low spin at low temperature and exists in a thermal equilibrium of high- and low-spin forms at room temperature. Higher temperatures would be

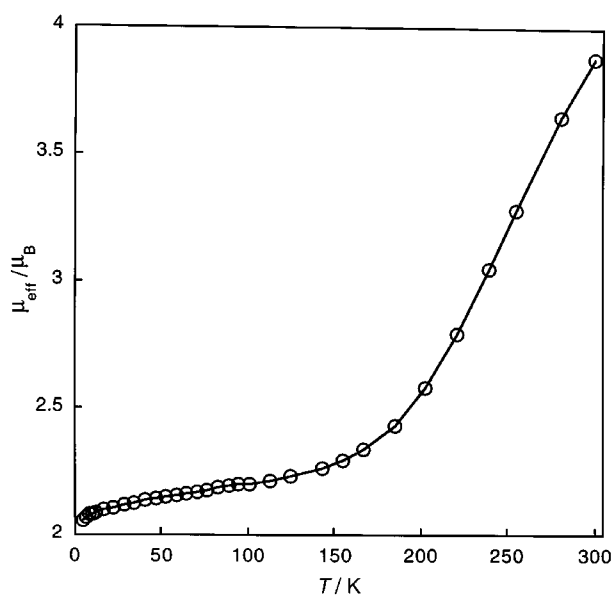
Table 2 Selected bond distances (Å) and angles (°) in [Cr(dmptacn)Cl][ClO₄]₂

Cr(1)–N(1)	2.047(6)	Cr(1)–N(5)	2.065(5)	Cr(2)–N(8)	2.056(5)
Cr(1)–N(2)	2.073(5)	Cr(1)–Cl(1)	2.295(2)	Cr(2)–N(9)	2.061(5)
Cr(1)–N(3)	2.058(5)	Cr(2)–N(6)	2.055(6)	Cr(2)–N(10)	2.065(5)
Cr(1)–N(4)	2.062(5)	Cr(2)–N(7)	2.072(5)	Cr(2)–Cl(2)	2.298(2)
N(3)–C(4)	1.521(9)	N(2)–C(3)	1.492(8)	N(7)–C(25)	1.499(9)
N(3)–C(5)	1.509(10)	N(2)–C(7)	1.492(8)	N(8)–C(22)	1.507(8)
N(3)–C(13)	1.467(10)	N(5)–C(14)	1.346(7)	N(8)–C(23)	1.503(10)
N(4)–C(8)	1.368(8)	N(5)–C(18)	1.339(9)	N(8)–C(31)	1.471(9)
N(1)–C(1)	1.486(8)	N(6)–C(19)	1.484(9)	N(9)–C(26)	1.357(9)
N(1)–C(6)	1.508(9)	N(6)–C(24)	1.493(10)	N(9)–C(30)	1.350(9)
N(4)–C(12)	1.350(8)	N(7)–C(20)	1.515(8)	N(10)–C(32)	1.349(9)
N(2)–C(2)	1.522(10)	N(7)–C(21)	1.494(8)	N(10)–C(36)	1.329(9)
N(2)–C(3)	1.492(8)				
Cl(1)–Cr(1)–N(1)	91.4(2)	N(6)–Cr(2)–N(8)	84.1(2)	Cr(1)–N(4)–C(8)	113.8(4)
Cl(1)–Cr(1)–N(2)	174.4(2)	N(6)–Cr(2)–N(9)	96.8(2)	Cr(1)–N(4)–C(12)	127.4(4)
Cl(1)–Cr(1)–N(3)	97.4(2)	N(6)–Cr(2)–N(10)	165.4(2)	Cr(1)–N(5)–C(14)	112.3(5)
Cl(1)–Cr(1)–N(4)	98.1(1)	N(7)–Cr(2)–N(8)	83.9(2)	Cr(1)–N(5)–C(18)	126.8(4)
Cl(1)–Cr(1)–N(5)	89.7(1)	N(7)–Cr(2)–N(9)	80.4(2)	Cr(2)–N(6)–C(19)	107.5(5)
N(1)–Cr(1)–N(2)	83.5(2)	N(8)–Cr(2)–N(9)	164.0(2)	Cr(2)–N(6)–C(24)	110.1(4)
N(1)–Cr(1)–N(3)	84.4(2)	N(8)–Cr(2)–N(10)	81.4(2)	Cr(2)–N(7)–C(20)	110.5(4)
N(1)–Cr(1)–N(4)	97.0(2)	N(9)–Cr(2)–N(10)	97.3(2)	Cr(2)–N(7)–C(21)	105.7(4)
N(1)–Cr(1)–N(5)	165.2(2)	Cr(1)–N(1)–C(1)	107.5(4)	Cr(2)–N(7)–C(25)	107.1(3)
N(2)–Cr(1)–N(3)	84.3(2)	Cr(1)–N(1)–C(6)	110.4(4)	Cr(2)–N(8)–C(22)	109.8(4)
N(2)–Cr(1)–N(4)	80.4(2)	Cr(1)–N(2)–C(2)	109.8(4)	Cr(2)–N(8)–C(23)	105.1(4)
N(2)–Cr(1)–N(5)	95.9(2)	Cr(1)–N(2)–C(3)	105.1(3)	Cr(2)–N(8)–C(31)	107.3(4)
N(3)–Cr(1)–N(4)	164.2(2)	Cr(1)–N(2)–C(7)	107.1(4)	Cr(2)–N(9)–C(26)	114.0(4)
N(3)–Cr(1)–N(5)	80.9(2)	Cr(1)–N(3)–C(4)	109.3(4)	Cr(2)–N(9)–C(30)	127.2(5)
N(4)–Cr(1)–N(5)	97.4(2)	Cr(1)–N(3)–C(5)	104.7(4)	Cr(2)–N(10)–C(32)	112.2(4)
N(6)–Cr(2)–N(7)	83.3(2)	Cr(1)–N(3)–C(13)	107.6(4)	Cr(2)–N(10)–C(36)	127.6(4)

Table 3 Physicochemical data for complexes of dmptacn and related ligands

Compound	$\mu_{\text{eff}}^a/\mu_{\text{B}}$	$\lambda_{\text{max}}/\text{nm}$ ($\epsilon/\text{dm}^3 \text{ mol}^{-1} \text{ cm}^{-1}$)	Ref.
[Cr(dmptacn)Cl][ClO ₄] ₂	3.98	506 (101), ^b 381 (104) ^b	This work
[Mn(dmptacn)(H ₂ O)][ClO ₄] ₂ ·H ₂ O	5.92		This work
[Fe(dmptacn)Cl][PF ₆] ₂ ·MeOH	3.58	530 (sh) (280), ^b 428 (1760), ^b 251 (12 070) ^b	This work
[Cr(tmptacn)][PF ₆] ₃	3.87	475 (134), 333 (106)	17
[Mn(tmptacn)][ClO ₄] ₂	5.82		17
[Fe(tmptacn)][ClO ₄] ₃	2.71	439 (408), 357 (sh) (960)	17

^a Measured at room temperature (295 K). ^b In MeCN.

**Fig. 3** Temperature dependence of the magnetic moment of [Fe(dmptacn)Cl][PF₆]₂·MeOH

needed fully to convert the complex into the high-spin form. The ESR spectrum in frozen dmf–MeOH solution displays a strong signal due to low-spin Fe^{III} with three *g* tensors,

$g_x = 1.96$, $g_y = 2.16$ and $g_z = 2.36$, and a weak signal at $g = 4.53$ which can be assigned to Fe^{III} in the high-spin ⁶A₁ state.^{9c} The room-temperature ESR spectrum of the powder, on the other hand, showed a single peak due to the high-spin form at $g = 4.52$. The ⁵⁷Fe Mössbauer spectrum shows three lines, a singlet superimposed on an asymmetric quadrupole doublet. At room temperature the doublet displays an isomer shift of $\delta = 0.18 \text{ mm s}^{-1}$ and a quadrupole splitting of $\Delta E_{\text{Q}} = 1.31 \text{ mm s}^{-1}$ which is indicative of low-spin Fe^{III}.²¹ The singlet at $\delta = 0.35 \text{ mm s}^{-1}$ with $\Delta E_{\text{Q}} \approx 0 \text{ mm s}^{-1}$ can be attributed to high-spin Fe^{III}. There are significant changes in the isomer shift and quadrupole splitting parameters on lowering the temperature, *vis-à-vis* at 77 K $\delta = 0.24 \text{ mm s}^{-1}$, $\Delta E_{\text{Q}} = 1.93 \text{ mm s}^{-1}$ while at 4.2 K $\delta = 0.23 \text{ mm s}^{-1}$, $\Delta E_{\text{Q}} = 1.90 \text{ mm s}^{-1}$. The Mössbauer peak areas suggest that the low-spin state comprises *ca.* 50% of the total Fe^{III} at room temperature and 70% at 77 K. Thus, the Mössbauer, ESR and magnetic susceptibility data all confirm that the complex is a spin-crossover system.

Electrochemistry

The redox behaviour of dmptacn complexes, studied by cyclic voltammetry in acetonitrile, is summarised in Table 4 along with data for closely related complexes. The [Cr(dmptacn)Cl]²⁺ complex exhibits a quasi-reversible one-electron Cr^{III}–Cr^{II} couple at -1.46 V indicating that the chromium(III) complex is a strong reductant. For [Cr(tmptacn)]³⁺ the same couple is observed at -1.88 V .¹⁷ Replacement of one pyridyl pendant

Table 4 Cyclic voltammetry data for complexes of dmptacn and related ligands

Couple	E_1/V	$\Delta E/mV$	i_{pa}/i_{pc}	Reversibility
$[\text{Cr}(\text{dmptacn})\text{Cl}]^{2+/+ a}$	-1.46	72 ^b	0.3	Quasi-reversible
$[\text{Mn}(\text{dmptacn})(\text{H}_2\text{O})]^{3+/2+ a}$	+0.41	66 ^b	1	Reversible
$[\text{Fe}(\text{dmptacn})\text{Cl}]^{2+/+ a}$	+0.35	76 ^b	0.67	Quasi-reversible
$[\text{Cr}(\text{tmptacn})]^{3+/2+ c}$	-1.88	120	≈ 1	Reversible
$[\text{Mn}(\text{tmptacn})]^{3+/2+ c}$	+0.77	245	—	Quasi-reversible
$[\text{Fe}(\text{tmptacn})]^{3+/2+ c}$	+0.35	70	≈ 1	Reversible
$[\text{Fe}(\text{dmpdaon})\text{Cl}]^{2+/+ d}$	+0.32 ^e	60	1	Reversible

^a Measured in MeCN, [complex] $\approx 10^{-3}$ mol dm⁻³ and 0.1 mol dm⁻³ NBu₄ClO₄, potentials are given relative to the ferrocene-ferrocenium couple, which was used as an internal standard ($E_1 = +0.435$ V). ^b Anodic to cathodic peak separations were determined at a scan rate of 100 mV s⁻¹. ^c Ref. 17. ^d Ref. 3. ^e +0.71 vs. Normal hydrogen electrode.

arm in tmptacn with a chloride ligand thus stabilises the chromium(II) state by ca. 420 mV. This indicates that the larger, Jahn-Teller distorted chromium(II) centre prefers to coordinate to the pentadentate dmptacn than to the hexadentate tmptacn. The smaller anodic-cathodic peak-potential separation observed for $[\text{Cr}(\text{dmptacn})\text{Cl}]^{2+}$ (72 mV) when compared with that for $[\text{Cr}(\text{tmptacn})]^{3+}$ (120 mV), suggests that the more flexible N₅Cl co-ordination sphere reorganises more readily than the N₆ system on reduction and oxidation.

In acetonitrile, $[\text{Mn}(\text{dmptacn})(\text{H}_2\text{O})]^{2+}$ exhibits a reversible Mn^{III}-Mn^{II} couple at +0.41 V which is less positive than that for $[\text{Mn}(\text{tmptacn})]^{2+}$ at +0.77 V.¹⁷ The greater stabilisation of the manganese(III) state by the dmptacn, compared with tmptacn, is in contrast to the Cr^{III}-Cr^{II} system where the chromium(II) state experiences greater stabilisation. It is possible that, following oxidation, Mn^{III} could be stabilised through deprotonation of the aqua ligand. In the case of the $[\text{Fe}(\text{dmptacn})\text{Cl}]^{2+}$ complex a quasi-reversible one-electron Fe^{III}-Fe^{II} process is observed at the same potential as that of the tmptacn complex (+0.35 V).¹⁷ Thus for these ligands there is no change in the relative stabilisation of either oxidation state. The related complex $[\text{Fe}(\text{dmpdaon})\text{Cl}]^+$ shows a reversible Fe^{III}-Fe^{II} redox process at +0.32 V under the same conditions.³ The only difference between the complexes is the substitution of the secondary amine in dmptacn for an oxygen atom in dmpdaon which results in stabilisation of the iron(III) state by ca. 30 mV. Although this correlates well with the higher affinity of Fe^{III} for oxo-donors, the high-spin nature of $[\text{Fe}(\text{dmpdaon})\text{Cl}]^+$ is also expected to influence the couple.

Acknowledgements

This work was supported by the Australian Research Council. G. A. M. was the recipient of an Australian Postgraduate Award.

References

- P. Chaudhuri and K. Wieghardt, *Prog. Inorg. Chem.*, 1987, **35**, 329; R. Bhula, P. Osvath and D. C. Weatherburn, *Coord. Chem. Rev.*, 1988, **91**, 89; L. F. Lindoy, *The Chemistry of Macrocyclic Ligands*, Cambridge University Press, Cambridge, 1989; P. V. Bernhardt and G. A. Lawrance, *Coord. Chem. Rev.*, 1990, **104**, 297.
- C. Flassbeck and K. Wieghardt, *Z. Anorg. Allg. Chem.*, 1992, **607**, 60.
- W. S. Szulbinski, P. R. Warburton, D. H. Busch and N. W. Alcock, *Inorg. Chem.*, 1993, **32**, 297.
- W. S. Szulbinski, P. R. Warburton and D. H. Busch, *Inorg. Chem.*, 1993, **32**, 5368.
- G. A. McLachlan, G. D. Fallon, R. L. Martin, B. Moubaraki, K. S. Murray and L. Spiccia, *Inorg. Chem.*, 1994, **33**, 4663.
- G. A. McLachlan, G. D. Fallon, R. L. Martin and L. Spiccia, *Inorg. Chem.*, 1995, **34**, 254.
- G. A. McLachlan, S. Brudenell, G. D. Fallon, R. L. Martin, L. Spiccia and E. R. T. Tiekink, *J. Chem. Soc., Dalton Trans.*, 1995, 439.
- S. J. Brudenell, L. Spiccia and E. R. T. Tiekink, *Inorg. Chem.*, 1996, **35**, 1974.
- See, for example, (a) A. J. Conti, R. K. Chadha, K. M. Sena, A. L. Rheingold and D. N. Hendrickson, *Inorg. Chem.*, 1993, **32**, 2670; (b) C. T. Brewer, G. Brewer, L. May, J. Sitar and R. Wang, *J. Chem. Soc., Dalton Trans.*, 1993, 151; (c) G. Brewer, J. Jasinski, W. Mahany, L. May and S. Prytkov, *Inorg. Chim. Acta*, 1995, **232**, 183 and refs. therein.
- P. Gütllich, *Struct. Bonding (Berlin)*, 1981, **44**, 83; E. König, *Struct. Bonding (Berlin)*, 1991, **76**, 51; H. Toftlund, *Coord. Chem. Rev.*, 1989, **94**, 67; P. Gütllich, A. Hauser and H. Spiering, *Angew. Chem., Int. Ed. Engl.*, 1994, **33**, 2024.
- G. D. Fallon and B. M. Gatehouse, *J. Solid State Chem.*, 1980, **34**, 193.
- G. M. Sheldrick, SHELX 76, Program for Crystal Structure Determination, Cambridge, 1976.
- J. A. Ibers and W. C. Hamilton (Editors), *International Tables for X-Ray Crystallography*, Kynoch Press, Birmingham, 1974, vol. 4.
- K. Wieghardt, U. Bossek, P. Chaudhuri, W. Hermann, B. C. Menke and J. Weiss, *Inorg. Chem.*, 1982, **21**, 4308.
- A. G. Orpen, L. Brammer, F. H. Allen, O. Kennard, D. G. Watson and R. Taylor, *J. Chem. Soc., Dalton Trans.*, 1989, S1.
- L. Christiansen, D. N. Hendrickson, H. Toftlund, S. R. Wilson and C.-L. Xie, *Inorg. Chem.*, 1986, **25**, 2813.
- K. Wieghardt, E. Schoffman, B. Nuber and J. Weiss, *Inorg. Chem.*, 1986, **25**, 4877.
- D. Sutton, *Electronic Spectra of Transition Metal Complexes*, McGraw-Hill, London, 1968; N. N. Greenwood and A. Earnshaw, *Chemistry of the Elements*, Pergamon, Oxford, 1984; A. P. B. Lever, *Inorganic Electronic Spectroscopy*, Elsevier, Amsterdam, 2nd edn., 1984.
- K. Wieghardt, W. Schmidt, W. Herrmann and H.-J. Küppers, *Inorg. Chem.*, 1983, **22**, 2953.
- K. Wieghardt, I. Tolksdorf and W. Herrmann, *Inorg. Chem.*, 1985, **24**, 1230.
- B. J. Kennedy, A. C. McGrath, K. S. Murray, B. W. Skelton and A. H. White, *Inorg. Chem.*, 1987, **26**, 483.

Received 3rd February 1997; Paper 7/00756F